Transaction B: Mechanical Engineering
Vol. 16, No. 4, pp. 332–343
© Sharif University of Technology, August 2009

SCIENTIA IRANICA

Effect of Payload Variation on the Residual Vibration of Flexible Manipulators at the End of a Given Path

M.H. Korayem[1,*], A. Heidari[1] and A. Nikoobin[1]

Abstract. *In rest-to-rest motion, the gripper of the flexible manipulators vibrates not only in the duration of the tracking but also after reaching the goal point. This vibration, which is called residual vibration, continues with a specific amplitude and frequency after reaching the goal point. In this paper, the effect of a carried payload on the residual vibration magnitude is investigated. The finite element method is employed for modeling and deriving the dynamic equations of the manipulator with flexible links and joints. Compared with previous works, the assumptions of low frequency and small amplitude of vibration about the final configuration are released and all terms in the dynamic equations are taken into account. Some simulations for a two-link flexible manipulator along two given paths are then performed for different payloads at the end-effector. In the first state, a polynomial-Fourier function is considered for joint motion and then a linear path for gripper motion. Finally, a straightforward approach for predicting the residual vibration amplitude, in terms of the payload, is proposed.*

Keywords: *Manipulator; Flexible link and joint; Residual vibration; Finite element method.*

INTRODUCTION

Most robotic manipulators are designed and built in such a manner to maximize stiffness in an attempt to minimize the system vibration and achieve good positional accuracy. High stiffness is commonly achieved by using heavy material. This, in turn, limits the speed of operation of the robot manipulation, increases the size of the actuator, boosts energy consumption and increases the overall cost. Flexible robot manipulators exhibit many advantages over rigid ones: They require less material, are lighter in weight, consume less power, require smaller actuators, are more maneuverable and transportable, have less overall cost and a higher payload to robot weight ratio [1]. However, due to the flexible nature of the system, the dynamics are highly non-linear and complex. Problems arise due to the lack of sensing, vibration due to system flexibility, imprecise positional accuracy and difficulty in obtaining an accurate model for the system [2]. The complexity of this problem increases dramatically when a flexible manipulator carries a payload. Practically, a robot is required to perform a single or sequential task such as picking up a payload, moving to a specified location or along a pre-planned trajectory and placing the payload. However, the dynamic behavior of the manipulator is significantly affected by payload variations, such that it can change the amplitude and frequency of the vibration. If the advantages associated with lightness are not to be sacrificed, we should have a comprehensive knowledge of their dynamic and vibratory behavior.

These vibrations can be divided into two parts: vibration along the path and the residual vibration after reaching the goal point. The residual vibration is caused by the residual kinetic and strain energy of the robot arm at the goal position. Due to its flexible nature, it vibrates and is not able to satisfy the desired path accurately; after reaching the end point this vibration continues. As a result, the robot manipulator needs some additional settling time after finishing each path and before starting a new one. Residual vibration can efficiently affect manipulator performance and efficiency during rest-to-rest motion or pick-and-place tasks. Various approaches have previously been developed for reducing residual vibration.

1. *Robotic Research Laboratory, College of Mechanical Engineering, Iran University of Science and Technology, Tehran, P.O. Box 16846, Iran.*
*. *Corresponding author. E-mail: hkorayem@iust.ac.ir*

Received 14 October 2007; received in revised form 14 May 2008; accepted 2 July 2008

Most work was based on either open-loop or closed-loop control strategies [3-6]. Residual vibration not only arises from system dynamic specifications but also depends on the path. In [7-9], residual vibration reduction is performed with the aid of path planning. As mentioned before, manipulator dynamical behavior depends considerably on payload mass. In [10], the effect of payload on vibration excitation along a path is studied and, in [11], the effect of payload changes on the resonance frequency of a single flexible link manipulator is considered; the effect of payload variation on residual vibration has not been considered up to now.

The suppression of vibration by the use of open loop control approaches or path planning methods is highly computational because of nonlinear, highly coupled and too lengthy equations. Furthermore, these methods frequently are combined with a close loop control strategy that necessitates the use of actuators and sensors that can work at high frequencies. Employment of these control methods requires the use of high speed computers, expensive sensors, actuators and other equipment. Therefore, using an open loop control without using the close loop control is more practical for a flexible robot manipulator, especially when a high accuracy in tracking or positioning is not needed.

In this paper, the effect of payload on the residual vibration of flexible robot manipulators at the end of the specified path is studied. The dynamic equation is derived by the Finite Element Method (FEM). One of the main advantages of FEM over most approximate solution methods is that the boundary conditions and the changes in geometry and physical properties can easily be considered to derive closed-form equations of motion. Unlike previous works, the flexibility in robot joints is considered in deriving the dynamic equations. Using the obtained equations, an approach is developed to determine the trajectory for a given path during the motion and after reaching the goal point. Additionally, all nonlinear terms are used to calculate residual vibration. Then, two simulations are performed for a two-link flexible manipulator along a linear path for the end effector and also for a combined Fourier-polynomial path for the joints. Then, these simulations are repeated for a flexible link and joint manipulator. Finally, using the obtained results, a new approach for prediction of the residual vibration amplitude, in terms of the payload mass, is presented.

MODEL DEVELOPMENT FOR A *N*-LINK FLEXIBLE MANIPULATOR

A multiple flexible link and joint manipulator consisting of m_{link} flexible links and m_{joint} flexible revolute joints is considered in the modeling (Figure 1). The authors in [12] have derived the dynamic equations of a flexible link manipulator using the finite element

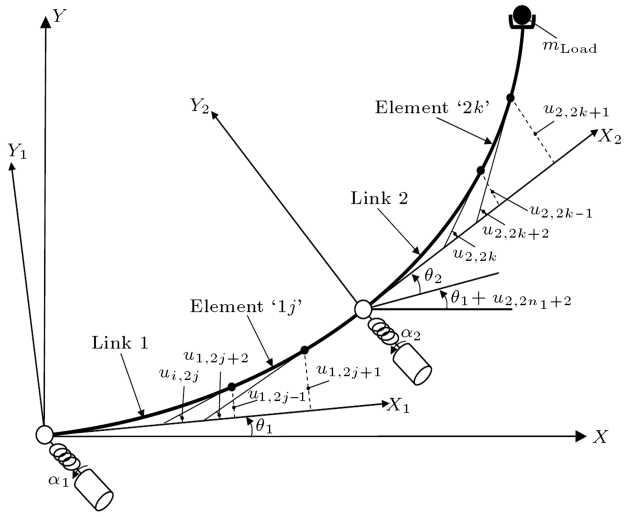

Figure 1. Schema of a two-link flexible manipulator.

approach without considering joint flexibility. In the present paper, flexibility is considered in both joints and links. The links are laid in a serial fashion and are actuated by rotors and hubs with individual motors. An inertial payload mass, m_L, is connected to the distal link. The proximal link is clamped and connected to the rotor with a hub.

Consider link i to be divided into elements '$i1$', '$i2$', ..., 'ij', $\cdots$ 'in_i' of equal length, l_i, where n_i is the number of elements of the ith link. Let us define the following notation, where subscript i refers to link i, and subscript ij refer to the jth element of link i. OXY is the inertia system of coordinates, $O_iX_iY_i$ is the body-fixed system of coordinates attached to link i. $u_{i,2j-1}$ is the flexural displacement at the common junction of elements '$i(j-1)$' and 'ij' of link i. $u_{i,2j}$ is the flexural slope at the tip of the common junction of elements '$i(j-1)$' and 'ij' of link i. This slope is measured with respect to axis O_iX_i.

For each element, kinetic energy, T_{ij} , and potential energy, V_{ij}, can be computed in terms of a selected system of generalized coordinates, q, and their rate of change with respect to time, $\dot{q}$. It is convenient to define r_i as the position vector of link i in the inertia reference frame in terms of the position of each point in the body-fixed coordinate system, $O_iX_iY_i$ (Figure 1), i.e.:

$$\vec{r}_1 = T_0^1 \begin{bmatrix} (j-1)l_1 + x_{1j} \\ y_{1j} \end{bmatrix},$$

$$\vec{r}_i = \left(T_0^1 \begin{bmatrix} L_1 \\ u_{2n_1+1} \end{bmatrix} + \cdots + T_0^1 T_1^2 \cdots T_{i-2}^{i-1} \begin{bmatrix} L_i \\ u_{2n_i+1} \end{bmatrix} \right) + T_0^1 T_1^2 \cdots T_{i-1}^{i} \begin{bmatrix} (j-1)l_i + x_{2j} \\ y_{2j} \end{bmatrix},$$

$$\text{for } i = 2, 3, \cdots \text{ NL (Number of Links)}, \qquad (1)$$

where T_{i-1}^{i} is the transformation matrix from $O_iX_iY_i$ to its previous body-fixed coordinate system. It is obvious that $O_0X_0Y_0 = OXY$ is the inertia system of coordinates.

$$T_0^1 = \begin{bmatrix} \cos\theta_1 & -\sin\theta_1 \\ \sin\theta_1 & \cos\theta_1 \end{bmatrix},$$

$$T_{i-1}^{i} = \begin{bmatrix} \cos(\theta_i + u_{2n_{i-1}+2}) & -\sin(\theta_i + u_{2n_{i-1}+2}) \\ \sin(\theta_i + u_{2n_{i-1}+2}) & \cos(\theta_i + u_{2n_{i-1}+2}) \end{bmatrix},$$

$$\text{for } i = 2, 3, \cdots \text{NL}, \tag{2}$$

where x_{ij} is the distance along O_iX_i in a body-fixed coordinate system from node $(j-1)$, l_i is the length of the elements in the ith link and θ_i is the joint angle between link i and $i-1$ (Figure 1). Finally, y_{ij} is defined as the element displacement and expresses the deformation of each link due to its original shape:

$$y_{ij} = \sum_{k=1}^{4} \phi_k(x_{ij}) u_{i,2j-2+k}(t), \tag{3}$$

where u is flexural displacement at the common junction of elements '$i(j-1)$' and 'ij' of link i and ϕ_k are the shape functions (Hermitian functions) of a beam element (Equation A1). Consequently, kinetic energy, T_{ij}, and potential energy, V_{ij}, for the jth element of link i can be computed by the following equation [12]:

$$T_{ij} = \frac{1}{2} \int_0^{l_i} m_i \left[\frac{\partial r_i^T}{\partial t} . \frac{\partial r_i}{\partial t} \right] dx_{ij}, \tag{4}$$

$$\begin{aligned} V_{ij} &= V_{gij} + V_{eij} \\ &= \int_0^{l_i} m_i g \begin{bmatrix} 0 & 1 \end{bmatrix} T_0^1 \begin{bmatrix} (j-1)l_i + x_{ij} \\ y_{ij} \end{bmatrix} dx_{ij} \\ &\quad + \frac{1}{2} \int_0^{l_i} EI_i \left[\frac{\partial^2 y_{ij}}{\partial x_{ij}^2} \right] dx_{ij}. \end{aligned} \tag{5}$$

As can be seen, potential energy consists of two parts. One part is due to gravity (V_{gij}) and another is related to the elasticity of the links, V_{eij}. These energies of elements are then combined to obtain the total kinetic energy, T, and potential energy, V, for each link. Total kinetic and potential energies of links are computed for a two-link robot in Equations A2 and A3. Knowledge of the kinetic and potential energies is needed to specify the Lagrangian $\pounds$ of the system, given by $\pounds = T - V$. The overall Lagrangian for a two-link flexible manipulator is calculated in Equation A4.

By replacing the selected system of a local generalized coordinate, q, applying Lagrange's equation, performing some algebraic manipulations and applying associated boundary conditions, the compact form of the dynamic equations becomes:

$$M(q)\ddot{q} + C(q, \dot{q}) + G(q) + Kq = \tau. \tag{6}$$

$M(q)$ is the manipulator configuration dependent generalized mass matrix, $C(q, \dot{q})$ considers the contribution of other dynamic forces such as centrifugal and Coriolis forces, while G is the vector of gravitational terms and K is the generalized structural stiffness matrix. Finally, τ is the vector of input torques (or forces) applied at the joints. The applied local generalized coordinate system, q, consists of all variables used in the modeling, as depicted in Figure 1:

$$\begin{aligned} q = \{&\theta_1, \theta_2, \cdots, \theta_m, u_{1,1}, u_{1,2}, \cdots, u_{1,2n_1+2}, \cdots, \\ &u_{m,1}, u_{m,2} \cdots, u_{m,2n_m+2}\}. \end{aligned} \tag{7}$$

The extension of the model to a case where a load, m_L, is added at the tip of the manipulator can be carried out by the mentioned approach. For computing kinetic and potential energies of the tip mass, position r_m can be expressed as follows:

$$\vec{r}_m = T_0^1 \begin{bmatrix} L_1 \\ u_{2n_1+1} \end{bmatrix} + \cdots + T_0^1 T_1^2 \cdots T_{i-2}^{i-1} \begin{bmatrix} L_i \\ u_{2n_i+1} \end{bmatrix},$$

$$\text{for } i = 2, 3, \cdots \text{NL}, \tag{8}$$

where u_{2n_i+1} is the flexural displacement of the of link i and L_i is the total length of this link. After computing the kinetic and potential energies of the tip mass from Equations 4 and 5, they can be added to the total energy of the robot in the Lagrangian of the system. Then, the matrix differential model of the overall system, with additional mass at the tip, can be derived through Lagrange equations [13].

On the other hand, Equation 6 can be separated and rewritten, based on rigid and flexible deformation variables, as follows:

$$M_{rr}\ddot{q}_r + M_{rf}\ddot{q}_f + C_{rr}\dot{q}_r + C_{rf}\dot{q}_f + G_r(q) = \tau, \tag{9}$$

$$M_{rf}\ddot{q}_r + M_{ff}\ddot{q}_f + C_{ff}\dot{q}_f + C_{fr}\dot{q}_r + G_f(q) + Kq_f = 0, \tag{10}$$

where $q_r = \{\theta_1, \theta_2\}$ and $q_f = \{u_{1,1}, \cdots, u_{1,2n_i+2}, \cdots, u_{m,1}, \cdots, u_{m,2n_m+2}\}$ are generalized joint position and flexible deformation variables, respectively, M_{rr} is the manipulator configuration dependent generalized mass matrix of the rigid part, M_{ff} is that of the flexible part, M_{rf} is that for the interaction of rigid and flexible variables, C_{rr}, and C_{ff} are the generalized matrix of Coriolis and centrifugal terms for rigid and flexible parts, respectively, C_{rf} and C_{fr} are those for the interaction of rigid and flexible variables, G_r and

G_f are the vector of gravitational terms for rigid and flexible parts, respectively, and K is the generalized structural stiffness.

Up to here, the dynamic model of a robot manipulator with flexible links and considering the payload at the end effector has been justified. For considering joint flexibility effects in dynamic simulations, the elasticity at the ith joint can be modeled as a linear torsional spring with spring constant, K_{ti}. According to Figure 2, α_i is representative of motor rotation, while θ_i shows joint rotation in modeling. By this assumption and using Equations 9 and 10, the dynamic equations of motion, considering both joint and link flexibility, will be changed as follows:

$$M_{rr}\ddot{q}_r + M_{rf}\ddot{q}_f + C_{rr}\dot{q}_r + C_{rf}\dot{q}_f + G_r(q) + K_t(q_r - q_{ac}) = 0, \quad (11)$$

$$M_{rf}\ddot{q}_r + M_{ff}\ddot{q}_f + C_{ff}\dot{q}_f + C_{fr}\dot{q}_r + G_f + Kq_f = 0, \quad (12)$$

$$I_r\ddot{q}_{ac} + K_t(q_{ac} - q_r) = \tau, \quad (13)$$

where $q_{ac} = \{\alpha_1, \alpha_2, \cdots, \alpha_m\}$ represent the motor angles, $K_t = \text{diag}\,[k_{t1}, k_{t2}, \cdots, k_{tm}]$ is the diagonal matrix of the restoring force constant, which models joint elasticity, $I_r = \text{diag}\,[I_{r1}, I_{r2}, \cdots, I_{rm}]$ is the diagonal matrix which represents motor inertia, and τ is the vector of the input torque applied by the actuators.

The above equations can be rearranged into the final form as below:

$$\begin{bmatrix} I_r & 0 & 0 \\ 0 & M_{rr} & M_{fr} \\ 0 & M_{fr} & M_{ff} \end{bmatrix} \begin{bmatrix} \ddot{q}_{ac} \\ \ddot{q}_r \\ \ddot{q}_f \end{bmatrix} + \begin{bmatrix} 0 & 0 & 0 \\ 0 & C_{rr}(q,\dot{q}) & C_{rf}(q,\dot{q}) \\ 0 & C_{fr}(q,\dot{q}) & C_{ff}(q,\dot{q}) \end{bmatrix} \begin{bmatrix} \dot{q}_{ac} \\ \dot{q}_r \\ \dot{q}_f \end{bmatrix} + \begin{bmatrix} 0 \\ G_r(q) \\ G_f(q) \end{bmatrix} + \begin{bmatrix} K_t & 0 & 0 \\ 0 & K_t & 0 \\ 0 & 0 & K \end{bmatrix} \begin{bmatrix} q_{ac} - q_r \\ q_r - q_{ac} \\ q_f \end{bmatrix} = \begin{bmatrix} \tau \\ 0 \\ 0 \end{bmatrix}. \quad (14)$$

CALCULATING THE RESIDUAL VIBRATION FOR A GIVEN PATH

Residual vibration, sustained after tracking the path, is the free oscillation of the manipulator with its natural frequencies of the final configuration depends on the initial condition. Here, displacement and velocity errors at final time t_f constitute initial conditions. In previous studies [9], by assuming the small deformation about the final configuration, centrifugal and Coriolis forces, which increased nonlinearity effects, were neglected. Considering these assumptions, the equations of motion in a flexible robot can be linearized; stopping the manipulator in the end point. In other words, the high order terms like q_f^2, $\dot{q}_f^2$, $q_f\dot{q}_f$, $q_f\dot{\theta}$ etc. can be ignored in the equations of motion. These assumptions are true when the residual vibrations about the final configuration have small amplitude and frequency. In this paper, all the above mentioned assumptions were violated and all non-linear terms were taken into account.

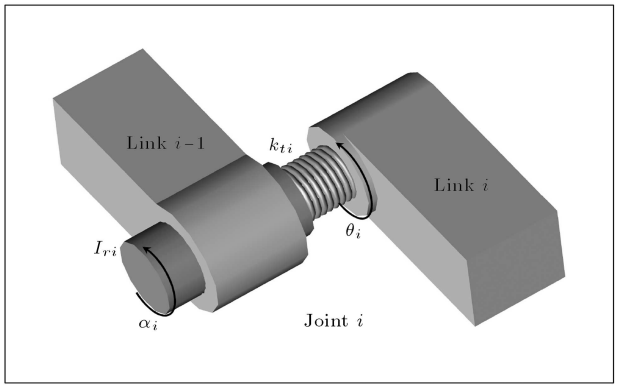

Figure 2. Schema of a flexible joint model.

There will be four possible situations for the solving of a robot manipulator depending on input.

Firstly, for flexible link-rigid joint manipulators, if joint trajectory is assumed as input, the values of q_r, $\dot{q}_r$ and $\ddot{q}_r$ will be the known parameters. Therefore, q_f can be calculated directly from Equation 10. These obtained values of q_f can then be used to calculate the joint torque with Equation 9.

Secondly, for the flexible link-rigid joint manipulators, if motor rotation, q_{ac}, is considered as input, the values of q_r and q_f can be derived by solving Equations 11 and 12 simultaneously. Correspondingly, the joint torque can be calculated from Equation 13.

On the other hand, if the gripper () moves along a pre-planned trajectory, the joints trajectory can easily be found from the inverse kinematic of a two-link robot with rigid joints and links.

The above-mentioned sets of equations are highly nonlinear and cannot be solved analytically; they should then be solved numerically in a state-space form. The flexible deformation variables can be considered as a vector:

$$15X = \begin{bmatrix} X_1 \\ X_2 \end{bmatrix} = \begin{bmatrix} q_f \\ \dot{q}_f \end{bmatrix}. \quad (15)$$

By this new definition of variables, Equation 10 can be rewritten in state-space form as:

$$\begin{cases} \dot{X}_1 = X_2 \\ \dot{X}_2 = -M_{ff}^{-1}(M_{rf}\ddot{q}_r + C_{fr}\dot{q}_r + C_{ff}X_2 + G_f \\ \qquad + KX_1) \end{cases} \tag{16}$$

Because q_r and $\dot{q}_r$ are two-valued functions (before and after t_f), Equation 16 should be solved in two steps: First, $0 \leq t \leq t_f$, for which the main path of the robot will be tracked and then, for $t > t_f$, it has residual vibration. Finally, for this case, the unknown generalized coordinates of robot (q_f) can be found from Equation 16.

Thirdly, for the flexible link and joint cases, for which the motor rotation, q_{ac}, is considered as input, the following variables can be defined:

$$X = \begin{bmatrix} X_1 & X_2 & X_3 & X_4 \end{bmatrix}^T = \begin{bmatrix} q_r & \dot{q}_r & q_f & \dot{q}_f \end{bmatrix}^T. \tag{17}$$

Equations 11 and 12 will change to the state-space form as:

$$\begin{cases} \dot{X}_1 = X_2, \dot{X}_3 = X_4 \\ \begin{bmatrix} \dot{X}_2 \\ \dot{X}_4 \end{bmatrix} = -\begin{bmatrix} M_{rr} & M_{fr} \\ M_{fr} & M_{ff} \end{bmatrix}^{-1} \left(\begin{bmatrix} C_{rr} & C_{rf} \\ C_{fr} & C_{ff} \end{bmatrix} \begin{bmatrix} X_2 \\ X_4 \end{bmatrix} \right. \\ \qquad \left. + \begin{bmatrix} G_r \\ G_f \end{bmatrix} + \begin{bmatrix} K_t & 0 \\ 0 & K \end{bmatrix} \begin{bmatrix} X_1 - q_{ac} \\ X_3 \end{bmatrix} \right). \end{cases} \tag{18}$$

Solving Equation 18, the generalized coordinates, $q = \{q_r, q_f\}$, can be computed. Finding these generalized coordinates is an introduction to determining the real trajectory, which has been tracked by the end-effector. Following this equation is another presentation of Equation 8 for the gripper position.

$$\begin{aligned} r_{fx} &= \sum_{k=1}^{m} (L_k \cos(\theta_k + u_{2n_{k-1}+2}) \\ &\quad - u_{2n_k+1} \sin(\theta_k + u_{2n_{k-1}+2})), \\ r_{fy} &= \sum_{k=1}^{m} (L_k \sin(\theta_k + u_{2n_{k-1}+2}) \\ &\quad + u_{2n_k+1} \cos(\theta_k + u_{2n_{k-1}+2})), \\ m &= 1, 2, \cdots \text{NL}. \end{aligned} \tag{19}$$

The desired path for a rigid robot can be expressed using the kinematic relation as follows:

$$\begin{aligned} r_{rx} &= \sum_{k=1}^{m} L_k \cos\left(\sum_{i=1}^{k} \theta_i\right), \\ r_{ry} &= \sum_{k=1}^{m} L_k \sin\left(\sum_{i=1}^{k} \theta_i\right), \\ m &= 1, 2, \cdots \text{NL}. \end{aligned} \tag{20}$$

Therefore, deviation from the desired path and the final point after t_f can be calculated by the following equations:

$$\begin{cases} e_x = r_{fx} - r_{rx}, & e_y = r_{fy} - r_{ry} \quad t \leq t_f \\ e_x = r_{fx} - x_f, & e_y = r_{fy} - y_f \quad t > t_f \end{cases} \tag{21}$$

where x_f and y_f represent the position of the gripper. Finally, the absolute value of the position error can be defined as:

$$P_e = \sqrt{e_x^2 + e_y^2}. \tag{22}$$

P_e represents the amount of deviation from the given path for $t \leq t_f$, on the one hand, and the amplitude of Residual Vibration (RV) for $t > t_f$ on the other. All mentioned procedures for computing gripper position, residual vibration and actuator torque in a flexible link and joint manipulator along a given path are outlined here:

Step 1 Specify the number of elements for each link and derive the dynamic equations by Equations 1 to 10 for the elastic link and Equations 11 to 13 for considering the flexibility of joints;

Step 2 Solve the inverse kinematic of a rigid robot to find q_r;

Step 3 Replace q_r in Equation 10 or q_{ac} (which is input) in Equations 11 and 12 then convert the variables using Equations 15 or 17 and rewrite the equations in the state-space form, as in Equations 16 or 18, for flexible link-rigid joint or flexible link-flexible joint cases, respectively;

Step 4 Solve Equations 16 and 18 numerically and find the unknown variables;

Step 5 Determine the simulated path of the gripper and calculate the amount of deviation from the tracked path and amplitude of residual vibration, using Equations 19 to 22;

Step 6 Compute the torque of actuators using Equations 9 or 13 for rigid or flexible joints.

SIMPLIFYING FOR TWO-LINK MANIPULATOR

Dynamic equations and required relations to calculate the residual vibration for a multiple flexible link and joint manipulator have been presented in the preceding sections. In this section, a two-link manipulator is considered and the above-mentioned equations are applied for this case. Considering two elements in each link ($n = 2$) and using Equation 8, the position vectors

of the first and second links change as follows:

$$\vec{r}_1 = T_0^1 \begin{bmatrix} (j-1)l_1 + x_{1j} \\ y_{1j} \end{bmatrix},$$

$$\vec{r}_2 = T_0^1 \left[\begin{bmatrix} L_1 \\ u_{2n_1+1} \end{bmatrix} + T_1^2 \begin{bmatrix} (j-1)l_2 + x_{2j} \\ y_{2j} \end{bmatrix} \right], \qquad (23)$$

where transformation matrixes will be simplified as follows:

$$T_0^1 = \begin{bmatrix} \cos\theta_1 & -\sin\theta_1 \\ \sin\theta_1 & \cos\theta_1 \end{bmatrix},$$

$$T_1^2 = \begin{bmatrix} \cos(\theta_2 + u_{2n_1+2}) & -\sin(\theta_2 + u_{2n_1+2}) \\ \sin(\theta_2 + u_{2n_1+2}) & \cos(\theta_2 + u_{2n_1+2}) \end{bmatrix}. \qquad (24)$$

By substituting Equations 23 and 24 into Equations 4 and 5, respectively, potential and kinetic energies can be derived. Using the Lagrange method, dynamic equations can be derived. In this formulation, it is assumed that the first joint of link 1 is constrained to have no displacement and angular displacement due to body-fixed axis O_1X_1 (u_1 and u_2, respectively). It means that boundary variables u_1 and u_2 must be zero, i.e. $u_1(t) = 0$ and $u_2(t) = 0$. The first joint in link 2 is similarly constrained and has no displacement and angular displacement due to O_2X_2 (w_1 and w_2, respectively). Therefore, constraint variables w_1 and w_2 must be zero, i.e. $w_1(t) = 0$ and $w_2(t) = 0$. It must be considered that both links have angular displacements, θ_1 and θ_2 with their body-fixed axis. After applying these boundary conditions, dynamic equations in the form of Equations 9 and 10 are derived. After defining the variables, using Equation 15 as the state variables:

$$X = \begin{bmatrix} u_3 & u_4 & u_7 & u_8 & \dot{u}_3 & \dot{u}_4 & \dot{u}_7 & \dot{u}_8 \end{bmatrix}, \qquad (25)$$

the state-space form of the equation can be obtained for flexible link-rigid joint cases, according to Equation 16. For the flexible joint and link manipulator, the state variables are defined as follows:

$$X = \lfloor \ \theta_1 \quad \theta_2 \quad \dot{\theta}_1 \quad \dot{\theta}_2 \quad u_3 \quad u_4 \quad u_7 \quad u_8 \quad \dot{u}_3 \quad \dot{u}_4 \quad \dot{u}_7 \quad \dot{u}_8 \ \rfloor. \qquad (26)$$

The state-space form of the equations can similarly be obtained from Equation 18.

EFFECTS OF PAYLOAD ON RESIDUAL VIBRATION

In order to initially check the validity of the presented model for flexible manipulators, a simulation test is performed for a rigid link and joint state (i.e. high stiffness EI). The obtained results are in good agreement with the existing solution for two-link rigid robots.

Since for the purpose of calculating residual vibration, the driven equations are highly coupled and nonlinear, studying the effect of payload variation on residual vibration can be undertaken via a number of simulations. Here, the simulations are performed for two different paths. In the first, a polynomial-Fourier function is considered for joint motion and in the second, a linear path has been selected for the gripper motion.

Path 1: Polynomial-Fourier Function for Joint Motion

In this simulation, a two-link flexible link-rigid joint manipulator is considered at the first stage and, then, flexibility in the joints is added. Required physical parameters are given in Table 1. Parameters used in the simulation of a two-link robot and its path are depicted in Figure 3. Two elements are considered in each link for the finite element model.

The combined Polynomial-Fourier functions are considered for joints motions as follows:

$$\theta_k(t) = \sum_{j=0}^{4} \lambda_j^k t^j + a_0^k \cos\frac{\pi t}{t_f}. \qquad (27)$$

In the above equation, there are six unknown parameters altogether for each joint. Applying boundary conditions at the start and goal point of the path, these six unknown parameters can be found. Using i to represent a joint number, the kinematic constraints at both ends, i.e. at $t = 0$ and $t = t_f = 1.5$ seconds, are given by:

$$\theta_{i0}(0) = \theta_{i0}^d, \qquad \theta_{if}(t_f) = \theta_{if}^d,$$

$$\dot{\theta}_i(0) = \dot{\theta}_i(t_f) = \ddot{\theta}_i(0) = \ddot{\theta}_i(t_f) = 0; \qquad i = 1, 2. \qquad (28)$$

Table 1. Physical parameters of robot arm.

Link/Joint Number	Length of Link (m)	Mass of Link (kg)	Moment of Inertia (m^4)$\times 10^{-9}$	Modulus of Elasticity (GPa)	Spring Constant (N/m)	Inertia of Motor (kg.m^2)
1	1	5	5	200	10000	0.1
2	1	5	5	200	10000	0.1

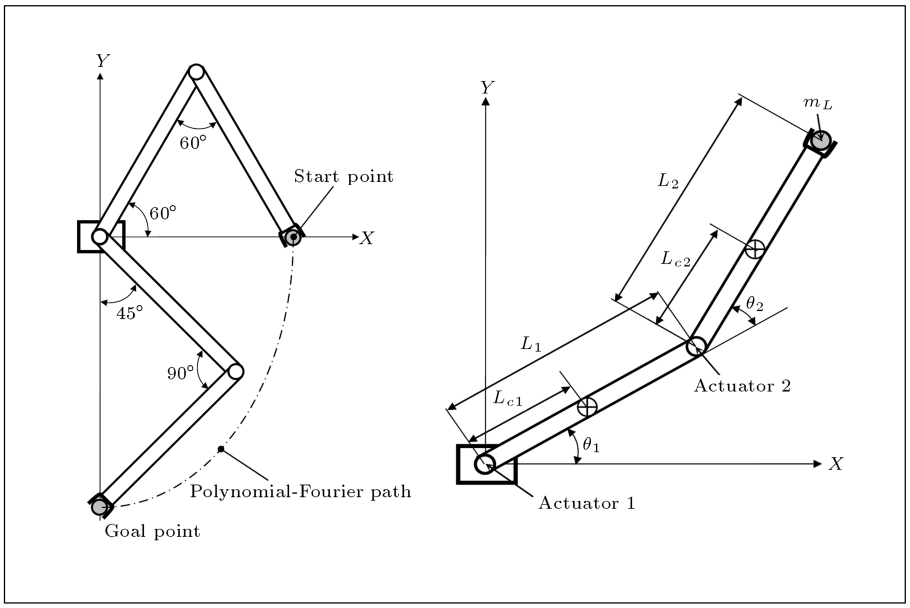

Figure 3. Parameters are used in two-link robot and its path.

The initial and final positions of the first and second joints, θ_{i0}^d and θ_{if}^d, are given as follows:

$$\theta_{10}^d = 60^\circ, \qquad \theta_{20}^d = -120^\circ,$$
$$\theta_{1f}^d = -45^\circ, \qquad \theta_{2f}^d = -90^\circ. \tag{29}$$

Vibration at the goal point has been measured for 1.5 seconds after stopping the manipulator at the goal point. The mentioned steps in the previous section can be applied to determine the Residual Vibration (RV). The desired and real path of a flexible link manipulator, considering gravity, are shown in Figure 4. A scaled view of the gripper vibration (at the goal point) is also represented. When the gripper reaches its goal point, the manipulator vibrates due to its residual energy. Residual vibration is depicted in Figure 5 for two different payloads, $m_L = 0,2$ kg. The residual vibrations can be placed in two circles, considering the goal point as their centre. The radius of these circles, R_i, which shows the maximum deviation of the gripper, can be used as a criterion for measuring residual vibration magnitude. R_1 and R_2 are the equivalent radius of residual vibration per $m_L = 0$ kg and $m_L = 2$ kg, respectively. It can be shown that the centre of the vibrations has a deviation, with respect to the goal point, due to gravity.

In order to study the effect of payload on the amount of residual vibration amplitude, a number of simulations have been done for different end-effector payloads and the relation between the radius of Residual Vibration (R_i) and the payload magnitude (m_L) has been depicted in Figure 6. Here, the flexible link manipulator with a Polynomial-Fourier function for

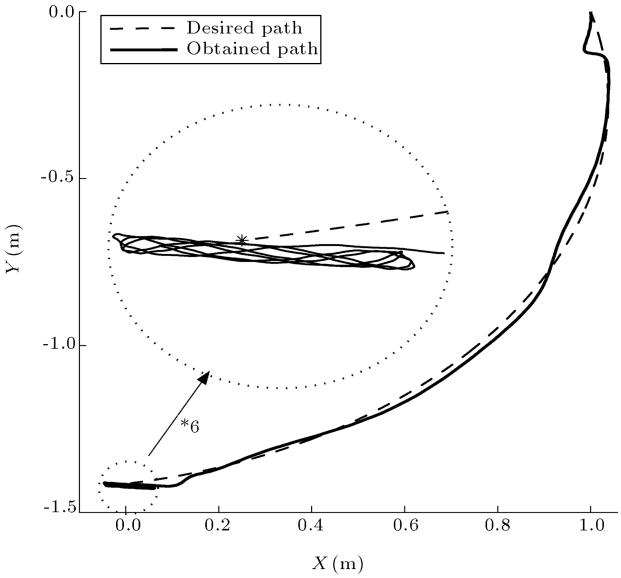

Figure 4. Desired and real path for $m_L = 2$ kg.

joint motion is considered. This simulation is repeated for a flexible link and joint manipulator and the results are shown in Figure 7. As can be seen from Figures 6 and 7, the RV rises generally by increasing the payload, except for a slight decrease in the second case. This decrease is due to the nonlinearity caused by flexibility in the joint.

Path 2: Linear Path

In this simulation, the gripper trajectory is linear which starts from point ($x_1 = 0$, $y_1 = 1$ m) and ends at a point with coordinates ($x_2 = 0.75$ m, $y_2 = 1.5$ m). The velocity profile of the end effector at each segment is as

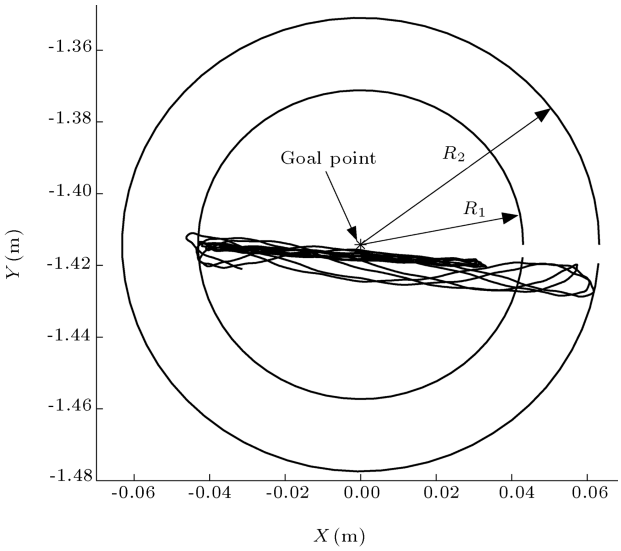

Figure 5. Radii of residual vibrations for $m_L = 0$, 2 kg.

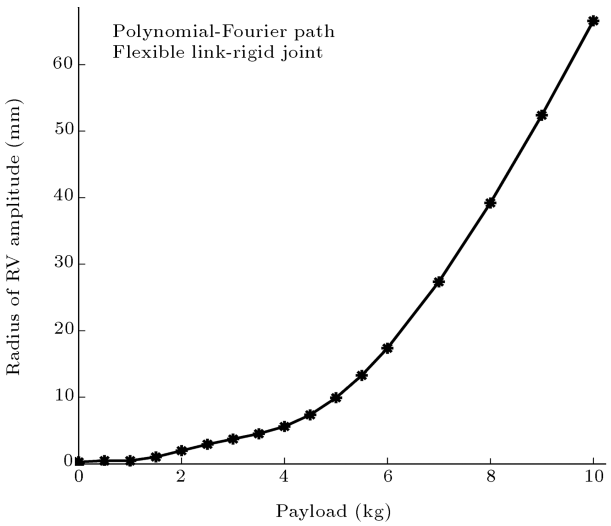

Figure 6. RV versus payload (flexible link-rigid joint).

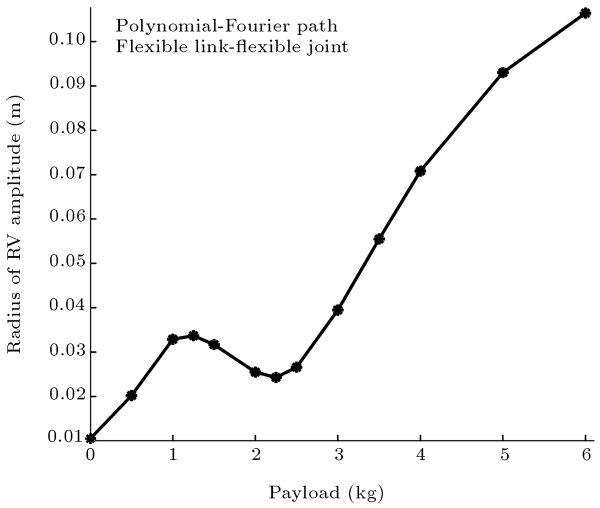

Figure 7. RV versus payload (flexible link and joint).

below:

$$\begin{cases} v = \text{at} & 0 \le t < T/4 \\ v = \text{at} & T/4 \le t < 3T/4 \\ v = -\text{at} & 3T/4 \le t \le T \end{cases} \tag{30}$$

where T is the overall motion time along the path equal to 1.452 seconds. The Residual Vibration is calculated for 1 second after stopping the robot at the goal point. Maximum velocity and acceleration of the are $V_{\max} = 0.75$ m/s and $a = 3$ m/s^2, respectively. Physical parameters of the simulation are similar to the first simulation (Table 1). Because the gripper path is predefined for this problem, an inverse kinematic should be firstly employed for determining the joint rotation. Afterwards, the real path and Residual Vibration can be achieved by the aforementioned procedure.

In Figure 8, the desired and tracked path of the end effector is depicted for the manipulator with a flexible link and $m_L = 2$ kg, and in Figure 9, the flexibility of the joints is also considered. As expected and easily seen in Figure 9, joint flexibility will increase the deviation along the path as well as the amplitude of the residual vibrations at the goal point.

The relation between the radius of the residual vibration and the amount of payload (m_L) is shown in Figures 10 and 11, for flexible link-rigid joint and flexible link-flexible joint manipulators, respectively, with a linear path. As expected, increasing the payload will increase the amplitude of the residual vibration. Also, the joints flexibility intensifies the deviation.

The amount of residual vibration amplitude is due to the residual kinetic and potential energies (strain energy in flexible joints and link) of the manipulator arm at the goal position. Because of the nonlinear relation between payload and residual vibration, to

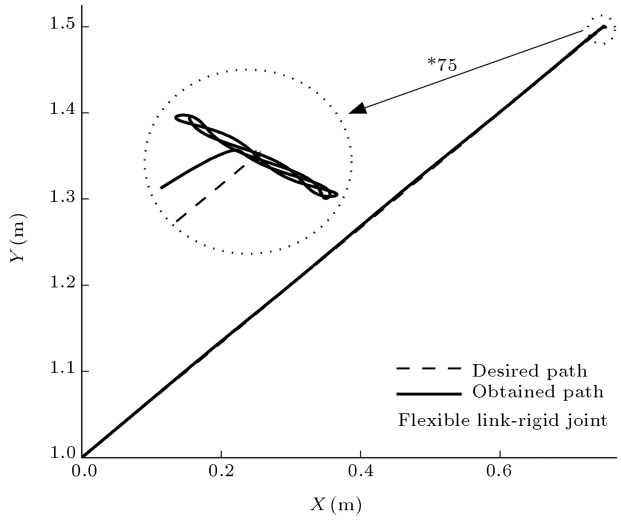

Figure 8. Desired and simulated path for $m_L = 2$ kg (flexible link-rigid joint).

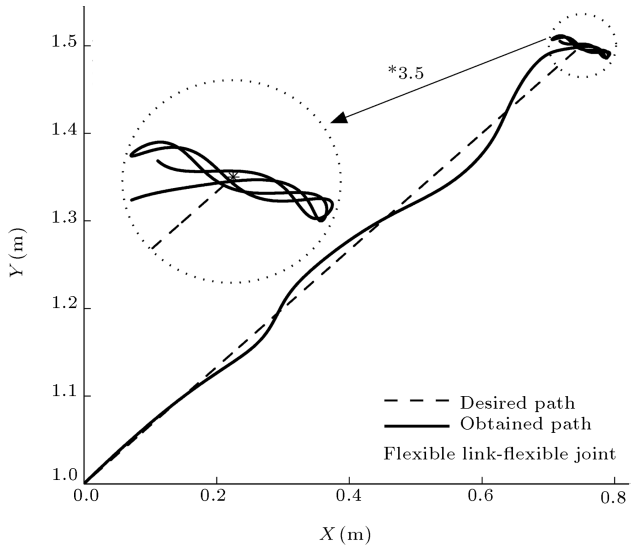

Figure 9. Desired and simulated path for $m_L = 2$ kg (flexible link-flexible joint).

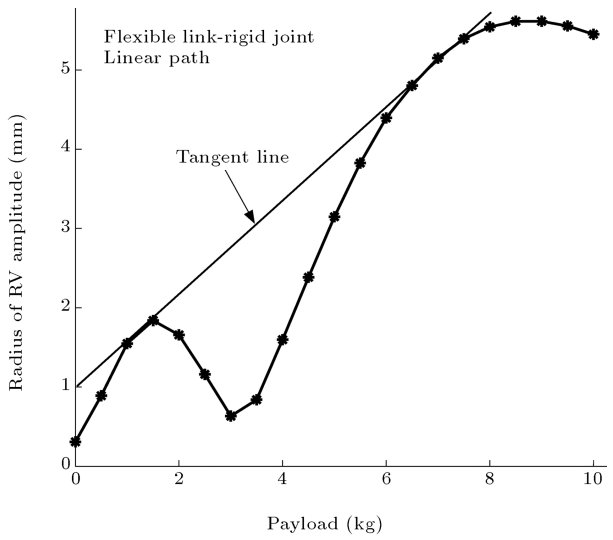

Figure 10. Effect of payload increment on deviations for flexible link-rigid joint.

estimate the variation of residual vibration amplitude in terms of payload value, a tangent line can be considered over the local maximum value of RV, as shown in Figures 10 and 11. This line can be used for estimating the amplitude of residual vibration with a negligible error. This line represents the maximum value of RV, which a flexible link and joint robot manipulator may have at the end of the given path with a specified payload.

CONCLUSION

In this paper, a new method for computing the residual vibration of a flexible manipulator is proposed and then the effects of the payload on the magnitude of

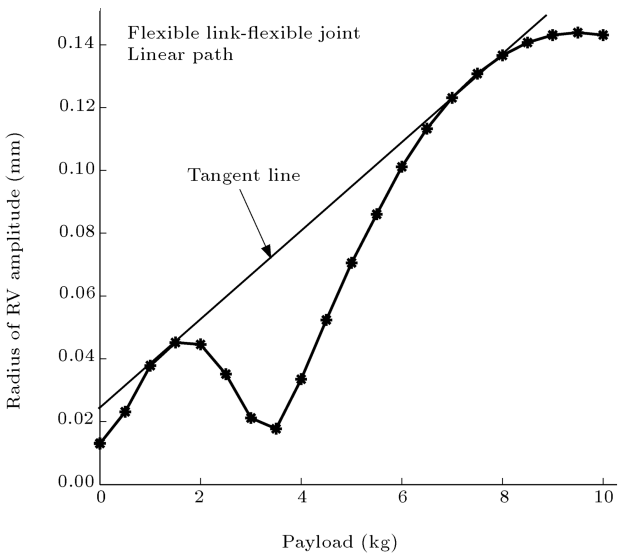

Figure 11. Effect of payload increment on deviations for flexible link-flexible joint.

the residual vibration are investigated. First, the FEM method is employed for modeling the flexible link manipulator and then, by considering the effects of the payload and also joint flexibility, the required relations are obtained. The solution of open loop dynamics has been tackled by decoupling the equation into rigid and flexible parts, which is well-known and effective in flexible manipulator dynamics. For predicting the relation between RV and the payload, a number of simulations are performed and, with good estimation, a tangent line has been found. Using this line, the maximum value of RV for a given payload can be estimated. The obtained results show that the overall trend of RV in a rigid joint-flexible link case is the same as in a flexible joint-flexible link case; joint flexibility just increases the amplitude of RV. Since in flexible link and joint robots the driven equations are highly coupled and too lengthy, an appropriate algorithm such as the presented procedure in this paper should be proposed for estimating RV for a given path and payload, without engaging in massive calculations. Using this algorithm, one can calculate the amount of error of the gripper for some payloads and estimate it for other values using the tangent line.

REFERENCES

1. Azad, A.K.M. "Analysis and design of control mechanisms for flexible manipulator systems", PhD Thesis, Department of Automatic Control and Systems Engineering, The University of Sheffield, UK (1995).
2. Piedboeuf, J.C., Farooq, M., Bayoumi, M.M., Labinaz, G. and Argoun, M.B. "Modeling and control of flexible manipulators - revisited", *Proc. of 36th Midwest Symposium on Circuits and Systems*, Detroit, pp. 1480-1483 (1993).

3. Mimmi, G., Frosini, L., Pennacchi, P. and Rottenbacher, C. "Open-loop control of a flexible manipulator with two links: Experimental results", *Proc. of the ASME Design Eng. Technical Conf.*, **6**, pp. 1969-1977 (2001).

4. Yan, A., Wang, G.-Q., Xu, H. and Sheng, Y. "Reduction of residual vibration in a rotating flexible beam", *Acta. Mechanica.*, **171**(3-4), pp. 137-149 (2004).

5. Yan, A., Xu, H., Cheng, J. and Sun, Y. "Hybrid control scheme for vibration suppression of a flexible manipulator", *Journal of Applied Mechanics*, **21**(4), pp. 62-66 (Dec. 2004).

6. Kermani, M.R., Moallem, M. and Patel, R.V. "Study of system parameters and control design for a flexible manipulator using piezoelectric transducers", *Smart Materials and Structures*, **14**(4), pp. 843-849 (2005).

7. Yue, S.G. "Redundant robot manipulators with joints and links flexibility II: Residual vibration decreasing", *Mech. Mach. Theory*, **33**(1-2), pp. 115-122 (1998).

8. Kojima, H. and Kibe, T. "Optimal trajectory planning of a two link flexible robot arm based on genetic algorithm for residual vibration reduction", *Int. Conf. on Intelligent Robots and Systems* (Nov. 3, 2001).

9. Park, K.J. "Flexible robot manipulator path design to reduce the endpoint residual vibration under torque constraints", *J. of Sound and Vibration*, **275**, pp. 1051-1068 (2004).

10. Tu, Q. and Rastegar, J. "Effects of payload on the vibrational excitation of robot manipulators during motion", *Proc. ASME Conf. Mach. Elements Mach. Dyn.*, pp. 17-24 (1994)

11. Tokhi, M.O., Mohamed, Z. and Shaheed, M.H. "Dynamic modeling of a flexible manipulator system incorporating payload: Theory and experiments", *Journal of Low Frequency Noise, Vibration and Active Control*, **19**(4), pp. 209-229 (2000)

12. Korayem, M.H, Heidari, A. and Nikoobin, A. "Maximum allowable dynamic load of flexible mobile manipulators using finite element approach", *Int. J. of Adv. Manuf. Technol.*, **36**, pp. 606-617 (2008)

13. Usoro, P.B., Nadira, R. and Mahil, S.S. "A finite element-lagrange approach to modeling lightweight flexible manipulators", *J. of Dynamic Systems, Measurement and Control*, **108**, pp. 198-205 (1986).

APPENDIX A

Model Development for a Two-Link Flexible Manipulator

This appendix is considered to show some undefined parts of the paper and also to describe how some parts of the general relation can be simplified. In Equation 3, the Hermitian function, $\phi_k(x_j)$, for a beam element is as below:

$$\varphi_1(x) = 1 - 3\left(\frac{x}{l}\right)^2 + 2\left(\frac{x}{l}\right)^3,$$

$$\varphi_2(x) = x\left[1 - 2\left(\frac{x}{l}\right) + \left(\frac{x}{l}\right)^2\right],$$

$$\varphi_3(x) = 3\left(\frac{x}{l}\right)^2 - 2\left(\frac{x}{l}\right)^3,$$

$$\varphi_4(x) = x\left[-\left(\frac{x}{l}\right) + \left(\frac{x}{l}\right)^2\right]. \quad \text{(A1)}$$

Kinetic Energy Computation

Total Kinetic Energy of Link 1

As link 1 is divided into n_1 elements, the total kinetic energy of link 1 is computed by adding over all element energies, '$1j$', of link 1 from Equation 4:

$$T_1 = \sum_{j=1}^{n_1} T_{1j} = \frac{1}{2}\dot{\tilde{q}}_1^T \tilde{M}_1 \dot{\tilde{q}}_1, \quad \text{(A2)}$$

where $\tilde{q}_1 = [\theta_1, \tilde{\psi}_1^T]^T$, $\tilde{\psi}_1 = [u_{1,11}\ u_{1,12}\ u_{1,13}\ u_{1,14}\ \cdots\ u_{1,2n_1-1}\ u_{1,2n_1}\ u_{1,2n_1+1}\ u_{1,2n_1+2}]^T$ and $\tilde{M}_1$ is the generalized inertia matrix of link 1.

Total Kinetic Energy for Link 2

The kinetic energy, T_2, of link 2 is computed by summing the elemental energies, T_{2j}, over all the second link, i.e.:

$$T_2 = \sum_{j=1}^{n_2} T_{2j} = \frac{1}{2}\dot{\tilde{q}}_2^T \tilde{M}_2 \dot{\tilde{q}}_2, \quad \text{(A3)}$$

where $\tilde{q}_2 = [\theta_1\ u_{1,2n_1+1}\ u_{1,2n_1+2}\ \theta_2\ \tilde{\psi}_2^T]^T$, $\tilde{\psi}_2 = [u_{2,1}\ u_{2,2}\ \cdots\ u_{2,2n_2+1}\ u_{2,2n_2+2}]^T$ and $\tilde{M}_2$ is the generalized inertia matrix of link 2.

Potential Energy Computation

The potential energy for the whole system is obtained by computing the potential energy for each element of the assemblage and adding them up overall.

Potential Energy for a Single Element '1j' of Link 1

Against kinetic energy, the mobility of the robot base does not add any extra term to the potential energy of the system; the potential energy of element '$1j$' of

link 1 only consists of gravity and elasticity in the links:

$$V_{1j} = V_{g1j} + V_{e1j}$$
$$= \int_0^{l_1} m_1 g \begin{bmatrix} 0 & 1 \end{bmatrix} T_0^1 \begin{bmatrix} (j-1)l_1 + x_{1j} \\ y_{1j} \end{bmatrix} dx_{1j}$$
$$+ \frac{1}{2} \int_0^{l_1} EI_1 \left[\frac{\partial^2 y_{1j}}{\partial x_{1j}^2} \right]^2 dx_{1j}. \quad \text{(A4)}$$

By substitution of y_{1j} from Equation A3 and taking the integrative (with respect to time) the elemental potential energy of link 1 becomes:

$$V_{1j} = \frac{1}{2} \psi_{1j}^T k_{1j} \psi_{1j} + m_1 g \begin{bmatrix} 0 & 1 \end{bmatrix} T_0^1$$
$$\begin{bmatrix} (j - \frac{1}{2}) l_1^2 \\ \frac{l_1}{2} u_{1,2j-1} + \frac{l_1^2}{12} u_{1,2j} + \frac{l_1}{2} u_{1,2j+1} - \frac{l_1^2}{12} u_{1,2j+2} \end{bmatrix}, \quad \text{(A5)}$$

where $\psi_{1j}^T = [u_{1,2j-1} \ u_{1,2j} \ u_{1,2j+1} \ u_{1,2j+2}]$ and K_{1j} is the stiffness matrix of the beam element.

Total Potential Energy for Link 1

Since link 1 comprises n_1 elements, its total potential energy is:

$$V_1 = \sum_{j=1}^{n_1} V_{1j} = m_1 g \begin{bmatrix} 0 & 1 \end{bmatrix} T_0^1 \begin{bmatrix} \frac{1}{2} n_1^2 l_1^2 \\ R_0 \tilde{\psi}_1 \end{bmatrix} + \frac{1}{2} \tilde{\psi}_1^T \tilde{K}_1 \tilde{\psi}_1, \quad \text{(A6)}$$

where $\tilde{\psi}_1$ is given in Equation A6 and $R_0 = \begin{bmatrix} l_1 & 0 \end{vmatrix} \begin{vmatrix} l_1 & 0 \end{vmatrix} \cdots \begin{vmatrix} l_1 & 0 \end{vmatrix} \frac{l_1}{2} \quad -\frac{l_1^2}{12} \end{bmatrix}$.

Potential Energy for a Single Element '2j'

Considering OX as the reference, the potential energy, V_{2j}, of jth element of link 2 is the sum of two components. One is due to gravity and the other is due to the elasticity of the system, i.e.

$$V_{2j} = \int_0^{l_2} m_2 g \begin{bmatrix} 0 & 1 \end{bmatrix} \left[T_0^1 \begin{bmatrix} L_1 \\ u_{1,2n_1+1} \end{bmatrix} + T_0^1 T_1^2 \begin{bmatrix} (j-1)l_2 + x_{2j} \\ y_{2j} \end{bmatrix} \right] dx_{2j}$$
$$+ \frac{1}{2} \int_0^{l_2} EI_2 \left[\frac{\partial^2 y_{2j}}{\partial x_{2j}^2} \right]^2 dx_{2j}$$
$$= m_2 g \begin{bmatrix} 0 & 1 \end{bmatrix} \left[T_0^1 \begin{bmatrix} L_1 \\ u_{1,2n_1+1} \end{bmatrix} l_2 + T_0^1 T_1^2 \right.$$
$$\left. \begin{bmatrix} \left(j - \frac{1}{2}\right) l_2^2 \\ \frac{l_2}{2} u_{2,2j-1} + \frac{l_2^2}{12} u_{2,2j} + \frac{l_2}{2} u_{2,2j+1} - \frac{l_2^2}{2} u_{2,2j+2} \end{bmatrix} \right]$$
$$+ \frac{1}{2} \psi_{2j}^T K_{2j} \psi_{2j}, \quad \text{(A7)}$$

where:

$$\psi_{2j}^T = [u_{2,2j-1} \ u_{2,2j} \ u_{2,2j+1} \ u_{2,2j+2}].$$

Total Potential Energy for Link 2

Summing over all elements, '2j', of link 2, the total potential energy of this link becomes:

$$V_2 = \sum_{j=1}^{n_2} V_{2j} = m_2 g \begin{bmatrix} 0 & 1 \end{bmatrix} \left[T_0^1 \begin{bmatrix} L_1 \\ u_{1,2n+1} \end{bmatrix} n_2 l_2 \right.$$
$$\left. + T_0^1 T_1^2 \begin{bmatrix} \frac{1}{2} n_2^2 l_2^2 \\ R_1 \psi_2 \end{bmatrix} \right] + \frac{1}{2} \tilde{\psi}_2^T K_2 \tilde{\psi}_2, \quad \text{(A8)}$$

where $\tilde{\psi}_2$ has been defined in Equation A7 and $R_1 = \begin{bmatrix} l_2 & 0 \end{vmatrix} \begin{vmatrix} l_2 & 0 \end{vmatrix} \cdots \begin{vmatrix} l_2 & 0 \end{vmatrix} \frac{l_2}{2} \quad -\frac{l_2^2}{12} \end{bmatrix}$.

Final Lagrangian of the Links

The overall Lagrangian for a two-link flexible manipulator can be written as:

$$\pounds = \pounds_1(\theta_1, u_{1,3}, u_{1,4}, \cdots u_{1,2n_1+2})$$
$$+ \pounds_2(\theta_1, u_{1,2n_1+1}, u_{1,2n_1+2}, \theta_2, u_{2,3},$$
$$u_{2,4}, \cdots u_{2,2n_2+2}). \quad \text{(A9)}$$

From Equations A2 and A6, the Lagrangian of the first link is as follows:

$$\pounds_1 = T_1 - V_1 = \frac{1}{2} \dot{q}_1^T M_1 \dot{q}_1 - m_1 g \begin{bmatrix} 0 & 1 \end{bmatrix} T_0^1 \begin{bmatrix} \frac{1}{2} n_1^2 l_1^2 \\ \\ R_0 \psi_1 \end{bmatrix}$$
$$- \frac{1}{2} \psi_1^T K_1 \psi_1. \quad \text{(A10)}$$

From Equations A3 and A8, the Lagrangian of link 2 can be derived:

$$\pounds_2 = \frac{1}{2} \dot{q}_2^T M_2 \dot{q}_2$$
$$- m_2 g \begin{bmatrix} 0 & 1 \end{bmatrix} T_0^1 \left[\begin{bmatrix} L_1 \\ u_{1,2n_1+1} \end{bmatrix} n_2 l_2 + T_1^2 \begin{bmatrix} \frac{1}{2} n_2^2 l_2^2 \\ \\ R_1 \psi_2 \end{bmatrix} \right]$$
$$- \frac{1}{2} \psi_2^T K_2 \psi_2. \quad \text{(A11)}$$

After computing the total kinetic and potential energies, the Lagrangian of the links of a flexible planar

two-link manipulator can be found:

$$\pounds_1 = T_1 - V_1 = \frac{1}{2}\dot{q}_1^T M_1 \dot{q}_1 - m_1 g \begin{bmatrix} 0 & 1 \end{bmatrix} T_0^1 \begin{bmatrix} \frac{1}{2} n_1^2 l_1^2 \\ R_0 \psi_1 \end{bmatrix} - \frac{1}{2}\psi_1^T K_1 \psi_1, \tag{A12}$$

$$\pounds_2 = T_2 - V_2 = \frac{1}{2}\dot{q}_2^T M_2 \dot{q}_2 - m_2 g \begin{bmatrix} 0 & 1 \end{bmatrix} T_0^1 \left[\begin{bmatrix} L_1 \\ u_{2n_1+1} \end{bmatrix} n_2 l_2 + T_1^2 \begin{bmatrix} \frac{1}{2} n_2^2 l_2^2 \\ R_1 \psi_2 \end{bmatrix} \right] - \frac{1}{2}\psi_2^T K_2 \psi_2, \tag{A13}$$

where:

$$q_1 = [\theta_1, \quad \psi_1^T]^T,$$

$$R_0 = [l_1 \quad 0 \big| \quad l_1 \quad 0 \big| \quad \cdots \big| l_1 \quad 0 \big| \quad \tfrac{l_1}{2} \quad -\tfrac{l_1^2}{12}],$$

$$\psi_1 = [u_{1,1} \quad u_{1,2} \quad u_{1,3} \quad u_{1,4} \cdots \quad u_{1,2n_1-1} \quad u_{1,2n_1} \quad u_{1,2n_1+1} \quad u_{1,2n_1+2}]^T,$$

$$q_2 = [\theta_1 u_{1,2n_1+1} \quad u_{1,2n_1+2} \quad \theta_2 \quad \psi_2^T]^T,$$

$$R_1 = [l_2 \quad 0 \big| \quad l_2 \quad 0 \big| \cdots \quad l_2 \quad 0 \big| \quad \tfrac{l_2}{2} \quad -\tfrac{l_2^2}{12}]$$

$$\psi_2 = [u_{2,1} \quad u_{2,2} \quad \cdots u_{2,2n_2+1} \quad u_{2,2n_2+2}]^T,$$

M_1 and M_2 are the general mass matrices of the first and second links, respectively, while K_1 and K_2 are the stiffness matrices of these two links [13].